Indonesian Journal of Science & Technology

Journal homepage: http://ejournal.upi.edu/index.php/ijost/

Numerical Simulation of Deep Mixed Columns Beneath the Heavy-Haul Railway Embankment

Hayder A. Hasan[1,], Khitam A. Saeed[1], Sahar Al-Khyat[1], Hadi Khabbaz[2]*

[1]Mustansiriyah University, Baghdad-Iraq
[2]University of Technology Sydney, Sydney, Australia
*Correspondence: E-mail: Hayder.Hasan@uomustansiriyah.edu.iq

ABSTRACT

One approach used to modify loose sand settlement under railway embankment involves deep mixed columns (DMCs). The geometrical properties of DMCs, such as the length, diameter, and spacing between adjacent columns, affect the distribution of load, failure mechanism, and ultimate resistance of a foundation constructed above soil reinforcement by this method. Numerical analysis is used as an alternative to laboratory modelling to minimize the cost and simplify the creation of complex DMC geometries in the lab. In this research, 3D Plaxis models are used to examine the influence of DMCs constructed under the embankment of a heavy-haul railway. The model used in this study has been calibrated and adjusted based on historical data from experimental tests on silty sand with low relative density. The study results offer details on how the bearing capacity of loose soil below train embankments is affected by the length and spacing of columns under static and dynamic loads.

ARTICLE INFO

Article History:
Submitted/Received 21 Feb 2025
First Revised 19 Mar 2025
Accepted 19 May 2025
First Available Online 20 May 2025
Publication Date 01 Sep 2025

Keyword:
Deep Mixed Columns,
Heavy-Haul Railway,
Moving load,
Numerical modelling.

1. INTRODUCTION

Deep Mixed Columns (DMCs) are a technique commonly used around the world to overcome the limitations of ground improvement by modifying the bearing capacity and minimizing the settlement of problematic soils. [1]. DMCs are implemented using two methods depending on the water content of the natural soil. The first technique is known as a dry method. In this process, the binder is injected into the soil using compressed air. However, the second method is called the wet method. In this process, the binder is added to the soil with water [2-3].

Although the common use of DMCs is carried out in soft clay soils, there have been limited studies dealing with using DMCs to enhance the efficiency of loose sandy soil. The influence of the density of sand soil, the percentage of the water-to-cement ratio for injecting slurry, and the number of blades on a drilling auger were investigated [4]. The outcome of the study showed that the compressive strength and modulus of elasticity displayed negligible increases with changes in density. In contrast, the performance of using augers with six blades is better than that of blades with four. It was also found that the strength and deformability were largest when the water-to-cement ratio was 1%, compared with 0.8% and 1.3%. Finally, the study involved statistical analysis using density, the ratio of water to cement, and curing time. Two equations were obtained to evaluate the strength and modulus of sand-cement mixing. The equations could be utilized to predict the performance of DMCs in loose sand.

Due to the poor engineering properties of marine and desert soils, constructing pavements on sandy subgrades is a considerable concern for geotechnical engineers, primarily because of the low rates of strength and cohesion. The deep mixing method was employed to enhance pavement load capacity by varying cement and bentonite percentages [5]. The results of the tests revealed that the unconfined compressive strength (UCS), secant modulus (Es), and resilient modulus were increased when the bentonite ratio was raised and the cement was partially replaced. For example, the highest UCS values were observed with 5% bentonite and 20% partial cement replacement after 28 curing days.

The mechanical and geometrical specifications of columns have a notable influence on the schematic diagram depicting the load distribution of road or railway embankments over loose subgrades [6]. The study emphasized that the performance of using the triangular pattern of deep mixed columns is better than the square pattern. The crest settlement of embankment under the soil reinforced with a triangular outline was recorded at 12% compared to the results of unreinforced soil. However, it was reported at 40% when using the square outline compared to the results of unreinforced soil.

The impact of using DMCs with different diameters and spacings on the bearing capacity of estuarine deposits at a normally consolidated condition under a road embankment has been examined [7]. The results from the Plaxis software demonstrated that the relationship between the bearing capacity and the area replacement ratio could be estimated based on the spacing between the cement columns. The ultimate bearing capacity of a foundation constructed on fibrous peat soil reinforced by end-bearing cement deep mixing with various improvement area ratios was assessed [8]. The experimental and numerical results illustrated that the shear strength of the DMCs increased with an increase in the area improvement ratio, depending on the stress distribution in unreinforced and reinforced soil with DMCs. The performance of DMCs below a raft foundation treated with polymer as a supplementary material using Plaxis 3D was investigated [9]. The DMCs were modelled under different scenarios, including various lengths and formations, such as floating or end-bearing. The

DOI: https://doi.org/10.17509/ijost.v10i2.83905
p- ISSN 2528-1410 e- ISSN 2527-8045

results showed a considerable increase in vertical stress when using DMCs to support the sandy soil, irrespective of the addition of polymer.

A three-dimensional numerical model has been designed to explore the influence of heavy axle loads of a train (e.g., 32.5 tons) on the excess pore water pressure and the settlement of soft clay subgrades after reinforcement with DMCs [10]. The results demonstrated a significant reduction in excess pore water pressures and settlements for both static and cyclic loads when using soil mixing columns. Additionally, it was clarified that cyclic loading resulted in a notable increase in vertical displacements and excess pore water pressure compared to the results observed under static loading conditions. The interference effect between two adjacent high-speed trains on the settlement of a railway track using Plaxis 3D has been discussed [11]. Importantly, they found that interference affects the dynamic settlement of the railway track and the critical velocity. For example, when the spacing between adjacent trains is 1 m, the percentage in dynamic settlement is increased from 17 to 58% when changing the train velocity from 25 km/h to 450 km/h, respectively. In addition, the effect of critical velocity is slightly reduced when the distance between trains is extended from 5 to 10 m. A numerical analysis of the stability and deformation characteristics of a high-speed railway embankment constructed on soft clay was presented [12]. The study recommends using cement for soil subgrade to enhance the stability and reduce the settlement of the railway embankments. The interaction between a strip footing and silty sand soil improved by a group of DMCs has been investigated [13]. The results of a study showed that a considerable reduction in settlement could be achieved depending on the number and length of the DMCs. The study outcome displayed that a significant decrease in settlement could be obtained based on the number and length of the DMCs.

These studies provide critical insights into using DMCs to address the limitations of traditional soil improvement techniques. However, the application of DMCs on a silty sand soil modelled under rail embankments of heavy moving trains is addressed in this study.

2. METHODS

2.1. Track and Soil Embankments

The rail is a crucial component of the track as it provides a continuous path for the train wheels. The steel beam section UIC 60 is a widely used choice for rail construction. To maintain the rail at the correct level and alignment, prevent track movement, and distribute the load in the ballast layer, concrete sleepers of type B 70 are regularly employed [14]. **Table 1** presents the properties of both the rail and sleepers, which are modelled as beam elements. Data was taken from literature [15].

The engineering properties of the railway embankment were modelled. Data was taken from literature [12]. The embankment comprises ballast, sub-ballast, and subgrade layers, which serve to distribute the stress from the rail to the underlying ground soil. The assumed thickness of the ballast and sub-ballast layers is 0.5 m, while the subgrade layer is assigned a thickness of 1 m. **Table 2** provides details of the properties of these layers.

2.2. Soil and Deep Mixed Columns (DMCs)

The properties of silty sand soil and DMCs are presented in **Table 3**, based on the experimental study referenced [13]. These properties are incorporated into the 3D Plaxis model to obtain results that closely match those observed in the laboratory model.

DOI: https://doi.org/10.17509/ijost.v10i2.83905
p- ISSN 2528-1410 e- ISSN 2527-8045

Table 1. Rail and sleeper properties. Data was taken from literature [15].

Parameter	Rail	Sleeper
Cross-sectional area (m^2)	$7.7x10^{-3}$	$5.13x10^{-2}$
Unit weight (kN/m^3)	78	25
Young's modulus (MPa)	$200x10^3$	$36x10^3$
Moment of inertia around the second axis (I_3)	$3.055x10^{-5}$	0.0253
Moment of inertia around the third axis (I_2)	$5.13x10^{-6}$	$2.45x10^{-4}$

Table 2. Ballast, sub-ballast, and subgrade layers properties. Data was taken from literature [12].

Parameter	Ballast and sub-ballast	Subgrade soil
Material model	Mohr-Coulomb	Mohr-Coulomb
Drainage type	Drained	Undrained B
Bulk unit weight (kN/m^3)	14.93	22.34
Modulus of elasticity (MPa)	110	9.6
Poissons Ratio	0.3	0.3
c or Su (kPa)	31.4	173.8
ϕ°	65.4	--

Table 3. Silty sand soil and DMC properties. Data was taken from literature [13].

Parameter	Silty sand soil	DMC as
Set type	Soil and interface	Embedded beams
Material model (type)	Mohr-Coulomb	Elastic
Drainage type	Drained	
Unit weight (kN/m^3)	14.28	16*
Modulus of elasticity (MPa)	2.5*	$392\ x10^3$
Poisson Ratio	0.25*	
ϕ°	38	
Tskin, start, max (kN/m)		0
Tskin, end, max (kN/m)		600#
Fmax (kN)		700#

*Assumed value, # Calculated by Plaxis 3D

Figure 1 illustrates the layout and distribution of DMCs under the strip footing in the Plaxis program. The model is constructed based on the shape of the laboratory model presented in [13]. The Plaxis model scales the laboratory model dimensions by a factor of 100. To illustrate, in the laboratory model, the footing length measured 0.49 m, while in the 3D Plaxis model, it is extended to 49 m in the longitudinal direction. In contrast, the width in the experimental model was 1 m; the Plaxis model is designed with a width of 10 m. In addition, the DMCs are modelled as embedded beams with a 2.2 m diameter and a 10 m length. The strip footing is represented in the Plaxis model as a rigid plate with 1 m in thickness.

As you can see. The pattern of DMCs is modelled as two parallel rows in the longitudinal direction. Each line comprises five elements of DMCs with a centre-to-centre spacing of 9 m. In contrast, the distance from the edge DMCs to the border of the foundation in the longitudinal direction is 6.5 m. In the width direction, the spacing between adjacent DMCs is 5 m. The DMC elements are designed in five columns. However, the distance between the DMCs and the edge of the strip foundation is 2.5 m in the width direction. The total number of DMCs that are used in both the experimental model and the Plaxis model is 10 columns.

DOI: https://doi.org/10.17509/ijost.v10i2.83905
p- ISSN 2528-1410 e- ISSN 2527-8045

The Plaxis model combined a strip footing with dimensions of 100 m in length and 60 m in width. The model also extended to a depth of 30 m.

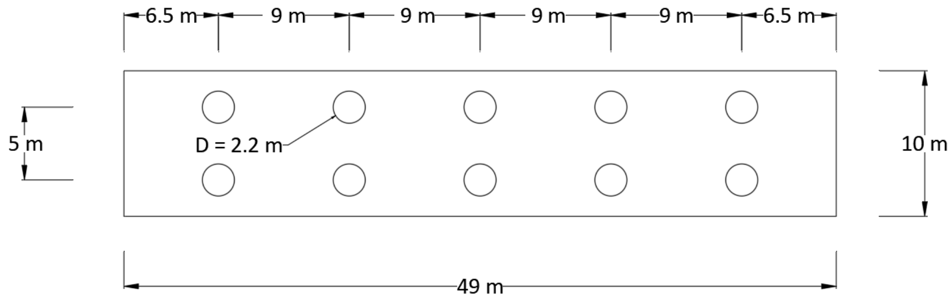

Figure 1. The dimensions of the strip footing with the arrangement and alignment of the cemented soil columns using Plaxis 3D.

Figure 2 illustrates the analysis of the stress versus settlement curves of the loose sand soil. The carves are recorded under two conditions: with and without soil reinforcement using ten DMCs of both numerical simulations using the Plaxis 3D and experimental model reported in [13].

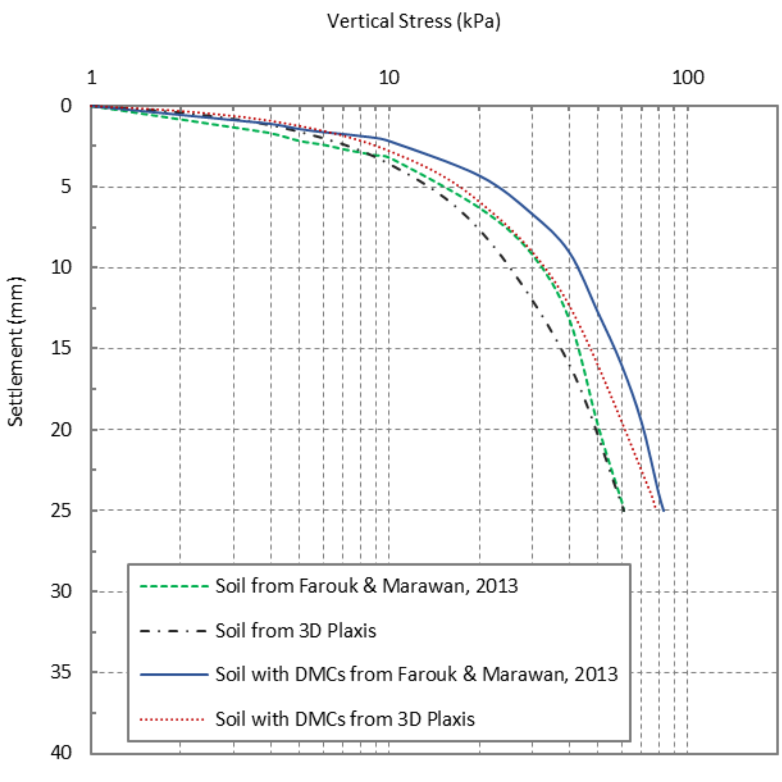

Figure 2. The stress versus settlement curves of soil with and without improvement by ten columns of soil–cement using the 3D Plaxis program and experimental model.

As shown, the comparison of the curves shows vertical stress plotted on the horizontal axis using a logarithmic scale. In contrast, settlement is plotted on the vertical axis using a linear scale. The relationship between stress and settlement in both experimental and numerical simulations, with and without soil reinforcement, shows nonlinear settlement that occurs under the compression stress of the soil. As the applied stress is low, the soil settlement

DOI: https://doi.org/10.17509/ijost.v10i2.83905
p- ISSN 2528-1410 e- ISSN 2527-8045

remains relatively minor. However, when the stress increases, the settlement increases rapidly.

Correlation and regression analyses are used to clarify the similarity in settlement under different stresses between experimental and numerical results for unreinforced and reinforced soil with DMCs. For the unreinforced and reinforced soils with DMCs, the Pearson correlation coefficients (r) between the experimental and numerical approaches are calculated as 0.99 and 0.75, respectively. These r values show a strong positive linear relationship between the experimental and numerical results. Additionally, the coefficient of determination (R^2) ranges from 0.98 to 0.65 for unreinforced and reinforced soil with DMCs, respectively. The R^2 value displayed that 98% and 65% of the difference in the settlement of the experimental results could be described by the settlement data recorded from Plaxis, respectively.

The results of statistical analyses indicate that the relationship between the settlement under a range of applied stresses from both methods is nearly identical. Due to this high level of similarity, the geotechnical properties derived from the experimental test could be interchangeable with those in the Plaxis model.

3. GEOMETRY AND DIMENSIONS OF MATERIALS

Figure 3 depicts the geometry section of the double-track railway with an embankment. The crest of the embankment length is designed with 9600 mm. The total height of the embankment, consisting of ballast, sub-ballast, and subgrade layers, is assumed to be 1500 mm above the natural ground level to minimize the effect of moving train loads. The embankment slope is defined by a ratio of 2 in horizontal to 1 in vertical (2:1). The centre of the concrete sleeper is located at 2500 mm from the centre line of the crest embankment. The distance between the edge of the concrete sleeper and the border of the crest embankment is 1000 mm. The concrete sleeper length measures 2600 mm, and there is a 500 mm spacing between sleepers. Both the ballast and sub-ballast have a thickness of 500 mm, while the subgrade thickness is 1000 mm. The standard railway gauge is assumed to be 1450 mm. Minimizing the distance between adjacent trains can reduce the cost of construction but may compromise the stability of the embankment. According to the Rail Industry Safety and Standards Board (RISSB), the minimum spacing between the centres of adjacent trains is 4 m. The distance between two tracks in this study is assumed as 5000 mm, measured from the centre of one to the centre of the one. A layer of geogrid, with a stiffness (EA) of 5000 kN/m, is placed 0.1 m above the pile heads to alleviate the effects of soil arching in a piled embankment under train movement.

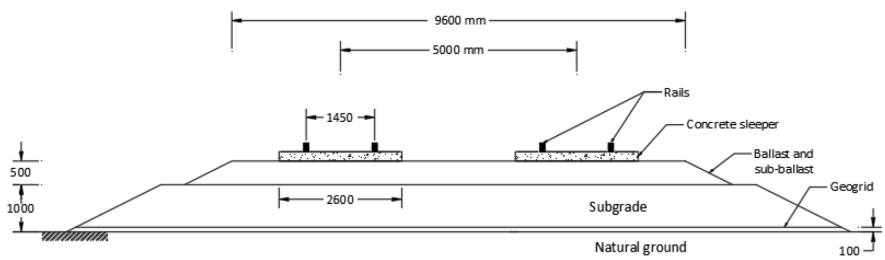

Figure 3. Geometry section of a double-track railway with an embankment.

DOI: https://doi.org/10.17509/ijost.v10i2.83905
p- ISSN 2528-1410 e- ISSN 2527-8045

Freight wagons, which are an essential part of current railway networks, are manufactured in a diverse range of dimensional characteristics to accommodate a varied range of cargo in different sizes and weights. The design of a freight wagon involves multiple phases, from process design to estimating and understanding the analysis results of the dynamic properties of moving loads affecting safety against derailments on twisted track, track loading, and running stability [16,17]. The length of heavy freight wagons, a fundamental factor in determining cargo carrying capacity, generally ranges from 12 to 15 m for hopper wagons according to the International Union of Railways (UIC) classification. Also, the distance between the traditional designs of bogies' centres varies from 8 to 12 m based on wagon length and cargo type. **Figure 4** displays the dimensions of a freight wagon used in this study. The wagon is assumed to consist of two bogies, each of which is supported by four axle loads. The length of the wagon is supposed as 15200 mm. In counters, the height is 3000 mm and the width is 3250 mm. The bogie centre is 11200 mm. The distance between wheel bases is 2000 mm, and the wheel diameter is 1000 mm. The distance between wagon to wagon from edge to edge is 1500 mm, while the far between the border wheel of the first wagon to the border of the second train is assumed to be 3700 mm. The axle load for any railway vehicle is defined as the mass transmitted onto the rails by a single wheel. The maximum allowable axle load for heavy haul rail can reach 32.5 tonnes when the train speed is limited to 80 km/h, according to [18]. In this study, the axle load is assumed to be 300 kN (~30 tonnes) with running speeds of up to 22.2 m/s (~80 km/h).

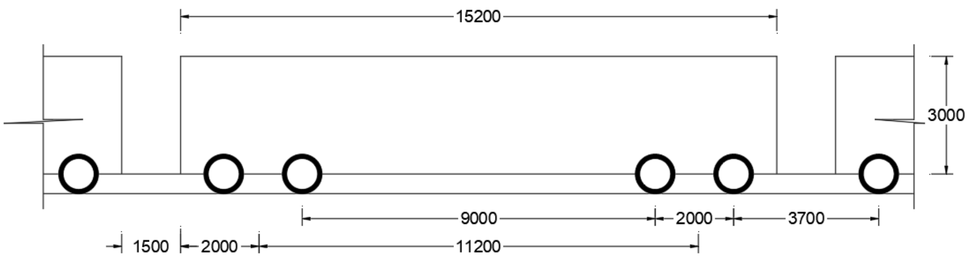

Figure 4. Dimensions of a freight wagon used in this study.

The DMC's layout is assumed to be square to investigate its impact on the bearing capacity of loose sandy soil. The study adopted the area replacement ratio (a_s) Technique, depending on literature [19], to determine the effect of DMC spacing. The expression of the area replacement ratio is formulated about the diameter (D) and spacing (S) of DMC as follows in Equation (1).

$$a_s = \frac{\pi}{4}\left(\frac{D}{S}\right)^2 \tag{1}$$

The DMC diameter has been modelled as 1 m, while the DMC spacings are varied from 2 and 3 m. **Table 4** shows the area replacement ratios for different spacings.

Table 4. Area replacement ratios of 2 and 3 m spacings.

Diameter (m)	Spacing (m)	a_s
1	2	0.196
1	3	0.087

DOI: https://doi.org/10.17509/ijost.v10i2.83905
p- ISSN 2528-1410 e- ISSN 2527-8045

4. NUMERICAL MODELLING

Figure 5 illustrates a three-dimensional model of a train load acting on tracks over an embankment. The model dimensions are 30 m in the X-direction, 50 m in the Y-direction, and 15 m in the Z-direction. The silty sand soil is simulated using the Mohr-Coulomb constitutive model under drained conditions. This soil layer extends from the ground surface to a depth of 15 m and has a unit weight of 14.28 kN/m³. Below this depth, the soil is assumed to be stiff and incompressible, serving as a natural boundary for the base of the model. The groundwater table is neglected in the simulation.

The DMCs are modelled as embedded beam elements (as piles) under elastic conditions, with a unit weight of 16 kN/m³. Each pile is assumed to have a diameter of 1 m. The length and spacing of the piles are treated as variable parameters, with lengths of 10 m (L10) and 15 m (L15), and spacings of 2 m (S2) and 3 m (S3). As the piles are placed beneath an embankment subjected to dynamic train loading, they are assumed to have free-end conditions at the base. The piles are further characterized by a unit weight of 16 kN/m³ and a modulus of elasticity of 392 × 10³ MPa.

When using DMCs to improve the soil under a train embankment, it is used a layer of geogrid is used within the embankment layer to mitigate potential soil arching. The geogrid layer is inserted into the embankment at 100 mm above the ground surface. The geogrid is modelled as an elastic material with an isotropic axial stiffness (EA) of 5000 kN/m.

The moving load is assumed to have a magnitude of 300 kN and move at a velocity of 22.2 m/s under a linear signal pattern. The mesh element distribution is defined as medium to balance computational efficiency and accuracy. A dynamic analysis is employed to simulate the moving load, which applies at 2-second intervals during the staged construction process. To prevent spurious wave reflections at the model boundaries, viscous boundary conditions are implemented in all directions except at the top boundary (Z-max).

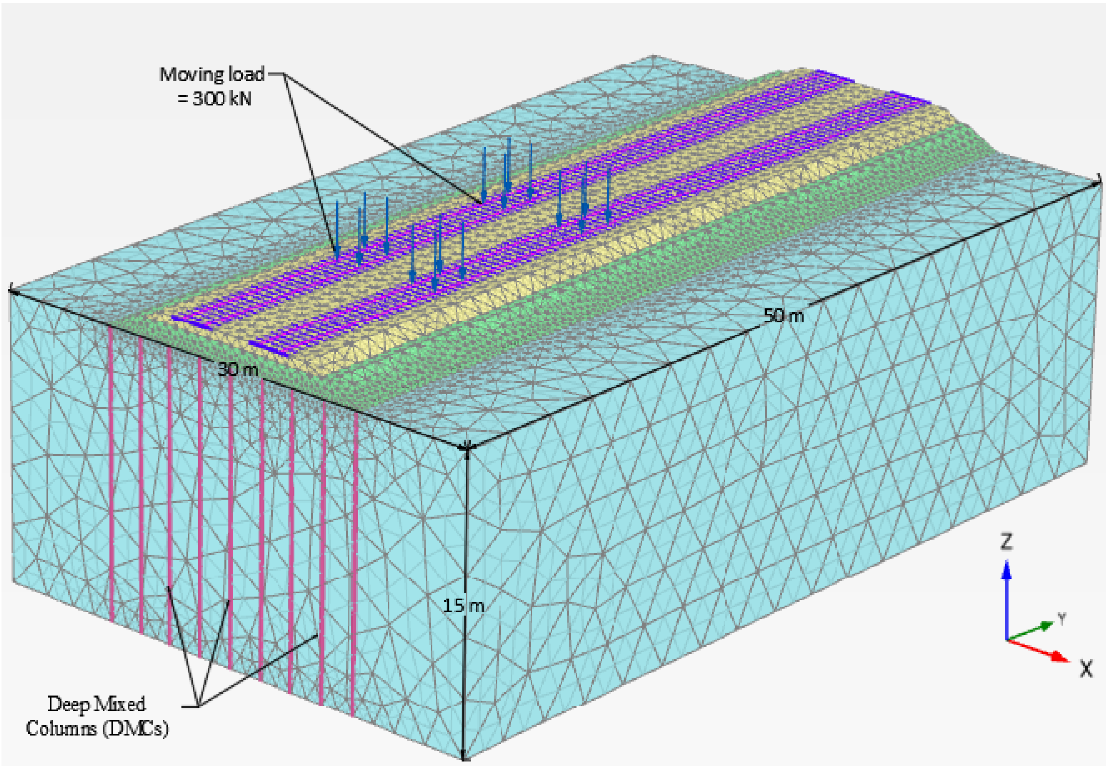

Figure 5. The 3D model of the train load in Plaxis 3D.

DOI: https://doi.org/10.17509/ijost.v10i2.83905
p- ISSN 2528-1410 e- ISSN 2527-8045

5. RESULTS AND DISCUSSIONS

5.1 The effect of static load on the settlement

The magnitude of the static load exerts a significant influence on the behaviour of the foundation system. It affects soil deformation, settlement, and the distribution of base pressure. **Figure 6** illustrates the relationship between static load and vertical settlement in unreinforced soil. The analysis is conducted by applying static loads representative of two trains at various positions along the track, at X = ±1.775 m and X = ±3.225 m, distribution of 12 m along the Y-axis. The loads apply under the rail line to assess the influence of spatial variability on soil settlement behaviour under uniform vertical loading. This approach has direct implications for determining the performance of the embankment layer and for optimizing the design of foundations for rail infrastructure.

The results indicate a linear increase in settlement with increasing static load across all positions. As expected, the vertical settlement magnitudes increase with increasing load intensity. However, the settlement values notably differ depending on the horizontal (X-axis) position of the applied load. That could be because of the presence of lateral heterogeneity within the subsurface soil conditions. Under a static load of 300 kN, the central loading positions (X = ±1.775 m) exhibit the largest magnitudes of settlement, with displacements reaching -116 mm at X = 1.775 m and -114 mm at X = -1.775 m. In contrast, the edge positions (X = ±3.225 m) display relatively lower settlement values of (-108 and -111 mm), respectively. The average settlement, inclusive of statistical standard error, is noted to range between -113.3 and -115.2 mm. These small differences in the results of the finite element modelling process could be attributed to the inherent discretization and approximations.

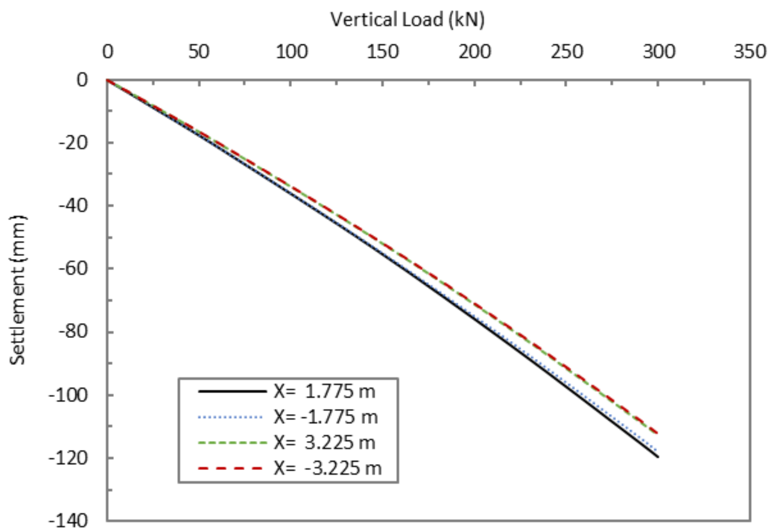

Figure 6. The relationship between static load and settlement of untreated soil at various locations in the X direction along 12 m in the Y direction under the rail of the train.

Figure 7 illustrates the settlement characteristics of unreinforced soil at varying depths along the vertical direction (Z-axis). The horizontal dimensions of the area under consideration are extended 1.775 m along the X-axis and 12 m along the Y-axis. The soil is subjected to a static load of 300 kN.

When the measurement is taken at the crest of the embankment (Z=1.5 m), the settlement is directly recorded under the railway rail, representing the immediate impact of the load. In contrast, when settlement measurement is taken at the natural ground level (Z = 0 m), the settlement reflects the soil response at the surface. The results reveal that with increasing

DOI: https://doi.org/10.17509/ijost.v10i2.83905
p- ISSN 2528-1410 e- ISSN 2527-8045

depth, the extent of soil settlement diminishes. For example, at a depth of 1.5 m along the Z-axis (embankment crest), a settlement of 119 mm is noted. With increasing depth, the settlement amount decreases to 106 mm at a 1 m depth, 99 mm at 0.5 m, and finally 95 mm at Z = 0 m (the surface of silty sand soil).

A modification of approximately 12% in the settlement ratio is noted when calculating the settlement at 0.5 m beneath the crest of the embankment (Z = 1 m) compared to the settlement at the embankment crest (Z = 1.5 m). In contrast, the largest reduction of 25 % is noted at a depth of 1.5 m below the crest (Z = 0 m). This phenomenon could be attributed to the classical soil behaviour under direct loading, such as Boussinesq's theory, which demonstrated that vertical stress decreases steadily with depth as the load distributes over an increasingly larger area.

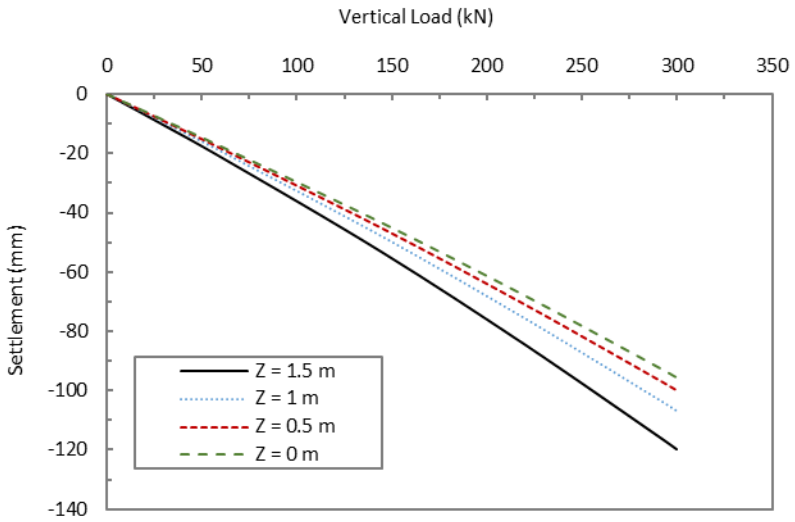

Figure 7. Soil settlement of untreated soil at different levels in the Z direction within 1,755 m in the X direction and 12 m in the Y direction.

The impact of static loading on the settlement of soil treated with DMCs is presented in **Figure 8**. The applied load is positioned along the rail track at 1.775 m in the X direction and 1.5 m in the Z direction. In the Y direction, the loads are set at 12 and 13 m for the DMC model with a length of 10 m and a centre-to-centre spacing of 2 m (L10S2). In contrast, the load is applied at 12 and 13.5 m in the Y direction for the DMCs model with a 3 m spacing between adjacent columns and the same length (L10S3).

The results demonstrate that settlement increases when the load is applied between columns. For instance, under the L10S2 composition, placing the load at 12 m in the Y direction, directly above a column, results in a settlement of 83 mm. However, when the load is shifted to 13 m, which places it between adjacent columns, the settlement increases to 86 mm. This increase highlights the influence of column positioning relative to the applied load.

Similarly, under the L10S3 configuration, a load positioned at 12 m in the Y direction generates a settlement of approximately 94 mm. In contrast, when the load is moved to 13.5 m (between adjacent columns), the settlement increases to 98 mm. This pattern confirmed that the settlement is more severe when the load is applied between DMCs. Therefore, the positioning of static loads to column alignment plays a critical role in controlling ground settlement.

DOI: https://doi.org/10.17509/ijost.v10i2.83905
p- ISSN 2528-1410 e- ISSN 2527-8045

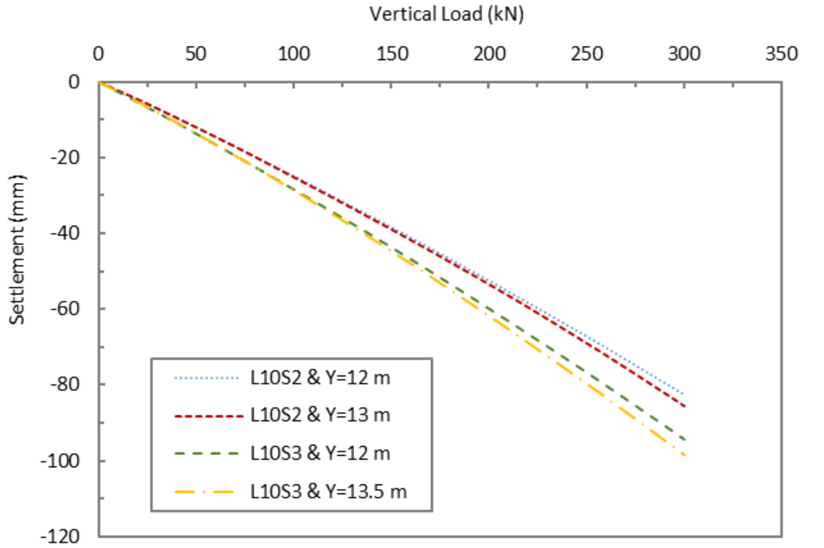

Figure 8. Effect of static load applied at various points along the Y-axis within a 1.775 m in the X-direction and a 1.5 m in the Z-direction on the settlement of soil reinforced with DSMs at 2 and 3 m spacing within a 10 m length.

Figure 9 illustrates the influence of static load placement on soil settlement for both unreinforced and reinforced soil with DMCs. In the unreinforced case, a settlement of 120 mm is reached under a vertical load of 300 kN, corresponding to a 0.4 settlement to load slope.

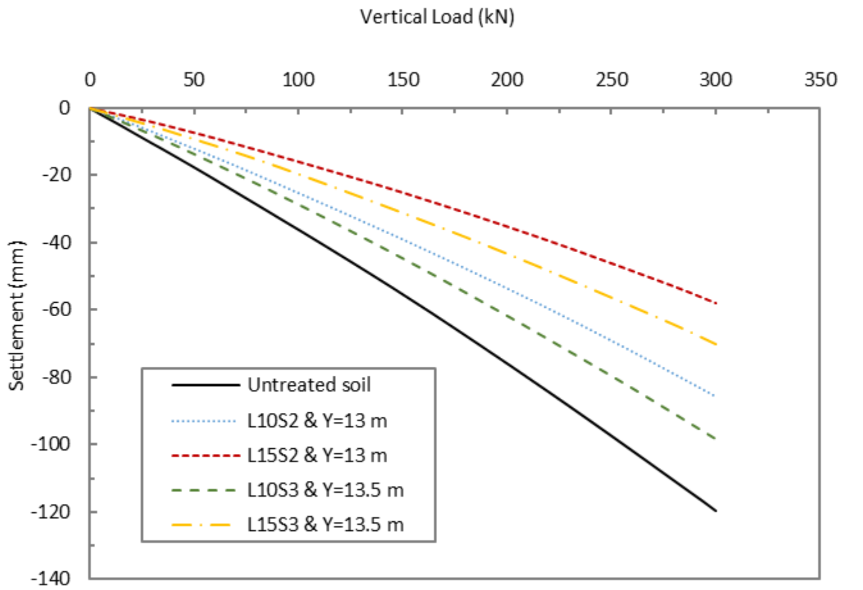

Figure 9. Effect of length and spacing on the settlement of soil for both untreated and treated with DMCs under static load conditions.

Modelling the DMCs with a 10-m length and a 3-m spacing between adjacent columns (L10S3) reduces the settlement to 98 mm, with an approximate slope of 0.33. However, further reducing the 2 m in spacing while maintaining a 10 m in length (L10S2) results in a settlement of 85 mm and an approximate slope of 0.28. This reduction could be related to an

DOI: https://doi.org/10.17509/ijost.v10i2.83905
p- ISSN 2528-1410 e- ISSN 2527-8045

increase in the ratio of area replacement, which directly affects minimizing the value of settlement [19].

Moreover, as the DMCs' length increases to 15 m, a lower settlement is recorded. When the modelling is designed with a pattern of 3 m (L15S3), the settlement decreases to 70 mm, presenting a slope of 0.23. In contrast, with modelling using a 2 m spacing (L15S2), a significant reduction in settlement to 58 mm is recorded, with a corresponding slope of 0.19. This settlement improvement when using the L15S2 model could be attributed to increased skin friction along the DMCs and also to the transition in the calculation of bearing capacity of the DMCs group from a floating stage to an end bearing state [9]. These results confirm the effect of length and spacing on the efficiency of DMCs in achieving effective ground improvement for railway infrastructure projects.

5.2. The Effect of Moving Load on the Settlement

The dynamic behaviour of soil under moving loads is a very complex phenomenon that is influenced by numerous factors, such as the magnitude and speed of the moving loads. Consequently, these factors considerably affect the settlement of soil. To investigate the influence of DMCs on soil settlement beneath a moving train, modelling data are selected along the railway track at X-axis positions of 1.775, -1.775, 3.225, and -3.225 m, with a fixed depth of 1.5 m in the Z direction. For a DMC spacing of 2 m, the Y-axis locations are set at 24 and 25 m; for a 3 m spacing, modelling conduct at 24 and 25.5 m. These locations (24, 25, and 25.5 m) are selected for vertical displacement calculations to ensure that settlement remains within acceptable limits under a 300 kN moving load travelling at a velocity of 22.2 m/s. The train movement is initiated from point 14 m in the Y direction, representing the initial location of the static load.

Figure 10 illustrates the relationship between soil settlement and dynamic time under a moving load on unreinforced soil at different positions along the X axis, with the Y axis fixed at 24 m and the Z axis depth set to 1.5 m. For detailed analysis, the rail at X = 1.775 m is selected. The dynamic settlement response reveals four distinct phases associated with the moving load of the train.

In the first phase, occurring between 0.0 and 0.3 seconds, settlement remains negligible, indicating minimal deformation before the arrival of the first axle. This suggests that the initial soil response is primarily elastic and unaffected by significant external load.

The second phase, between 0.3 and 0.6 seconds, shows a rapid increase in settlement. The soil is experiencing a settlement of -77 mm at 0.48 seconds under the first axle and -91 mm at 0.54 seconds beneath the second axle load. This 0.06-second interval corresponds to a 2 m axle spacing and confirms a train velocity of 22.2 m/s. Minor fluctuations in settlement between the two axles are caused by stress redistributions or wave reflections within the soil matrix.

During the third phase (0.6 to 1.0 seconds), the settlement curve exhibits a steady upward trend, suggesting a partial recovery of the soil surface. This behaviour could be attributed to stress wave interactions from the 9 m spacing between the second and third axles' loads. Following the fourth axle, the curve illustrates a significant uplift, indicating stress redistribution because of soil elasticity and dynamic interactions, and emphasizing the complexity of soil response under high-speed train movement.

Table 5 illustrates the effects of moving loads on the maximum settlement observed under various soil modelling scenarios along two adjacent railway tracks. As mentioned in the numerical modelling section, the first track is located at 1.775 and 3.225 m on the X-axis, while the second track is positioned at -1.775 and -3.225 m. The settlement on the inner rails of

DOI: https://doi.org/10.17509/ijost.v10i2.83905
p- ISSN 2528-1410 e- ISSN 2527-8045

both tracks (i.e., at 1.775 and -1.775 m) is greater than that of the outer rails (i.e., at 3.225 and -3.225 m) at Y = 24 m. For instance, settlements of 91 and 94 mm are recorded at 1.775 and -1.775 m, respectively, whereas the values decrease to 82 and 81 mm at 3.225 and -3.225 m, respectively. This trend could be attributed to the overlapping stress zones induced by the inner rails.

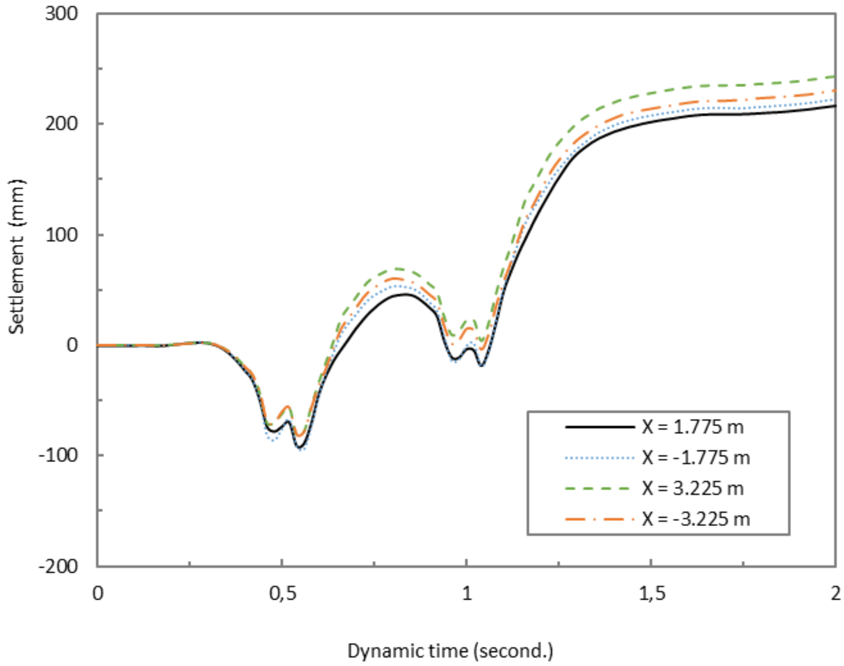

Figure 10. The impact of a moving train on soil settlement versus time without DMCs at a distance of 24 m in the Y direction and 1.5 m in the Z direction, with varying distances in the X direction.

Additionally, the average settlement along the X-axis is decreased from 87 mm in unreinforced soil to 54 mm in reinforced soil with DMCs 10 m in length and 2 m in centre-to-centre spacing of adjacent columns at the 24 m mark on the Y-axis. The impact of increasing DMC length is significantly illustrated in the magnitude of the Settlement Reduction Ratio (SRR). The SRR is increased from 38 to 50% as the DMC length increases from 10 to 15 m compared to unreinforced soil. This improvement could have resulted from enhanced skin friction and a transition from a floating to an end-bearing behaviour. In contrast, increasing the spacing between DMCs from 2 to 3 m results in reducing the SRR from 38 to 28% for 10 m columns, as well as from 50 to 32% for 15 m columns.

The SRR notably drops from 38 to 34% with a change in the Y-axis from 24 to 25 m, with the same modelling of DMCs, such as 10-m length and 2-m spacing. However, when modelling DMCs with a change in length to 15 m with steady spacing (2 m), the SRR is decreased from 50 to 46%. The lowest SRR value of 17% is observed when the DMCs are designed with a 10 m in length and a 3 m in spacing along the Y-axis equal to 25.5 m. Finally, with an increase in the column length to 15 m under the same spacing (3 m), the SRR is improved to 26% compared to unreinforced soil.

DOI: https://doi.org/10.17509/ijost.v10i2.83905
p- ISSN 2528-1410 e- ISSN 2527-8045

Table 5. Effect of soil modelling on the largest settlement of a moving train at various positions along the adjacent rail track of untreated soil.

Soil modelling	Y – Axis (m)	Settlement (mm)				Average settlement (mm)	Settlement reduction ratio (%) (SRR)
		X-axis					
		1.775	3.225	-1.775	3.225		
Soil	24	91	82	94	81	87	--
L10S2	24	58	52	53	53	54	38
L15S2	24	42	44	44	44	44	50
L10S3	24	64	60	65	63	63	28
L15S3	24	62	53	64	59	59	32
L10S2	25	60	54	58	56	57	34
L15S2	25	47	47	47	48	47	46
L10S3	25.5	76	68	75	71	73	17
L15S3	25.5	67	63	66	64	65	26

The dynamic response of unreinforced soil subjected to a moving axial load of 300 kN is analysed by examining vertical velocity fluctuations over time. These variations reflect soil deformation and recovery mechanisms as successive loads are applied. The data displays a cyclical pattern: an initial drop in vertical velocity caused by a moving train axle, followed by a rebound velocity due to the elastic and plastic responses of the soil, and then a gradual return to equilibrium. This is the behaviour of soil under dynamic loading conditions.

Figure 11 illustrates the relationship between vertical velocity and dynamic time for unreinforced soil beneath Rail 1, located at X = 1.775 m, under the influence of a moving train load. The analysis focuses on the vertical velocity response caused by a four-axle wagon, as depicted in **Figure 4**, with time intervals segmented according to axle passage, based on wheel spacing.

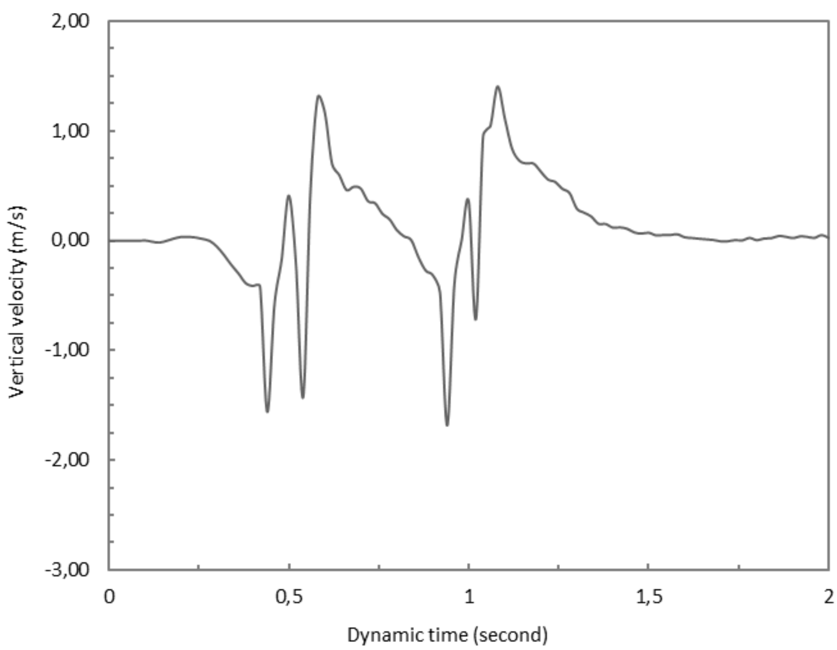

Figure 11: The impact of a moving train on vertical velocity in unreinforced soil under Rail 1 at X = 1.775 m.

DOI: https://doi.org/10.17509/ijost.v10i2.83905
p- ISSN 2528-1410 e- ISSN 2527-8045

The first axle load is applied at 0.44 seconds, producing a minimum vertical velocity of -1.56 m/s, indicating the maximum downward displacement and initial soil compression. This is followed by a rebound to 0.41 m/s at 0.5 seconds, resulting in a velocity amplitude of 1.97 m/s during the first loading cycle. The interval of 0.1 seconds between the first and second axles, corresponding to a 2 m wheel spacing, suggests insufficient recovery time for the soil before the next loading event.

When the second axle passes at 0.54 seconds, the vertical velocity reaches a minimum of -1.43 m/s, indicating slightly reduced compression compared to the first axle. The subsequent rebound at 0.58 seconds peaks at 1.31 m/s, resulting in an amplitude of 2.74 m/s exceeding that of the first cycle.

The third axle, impacting at 0.94 seconds, generates an amplitude of 2.05 m/s, with a minimum velocity of -1.69 m/s and then a rebound to 0.36 m/s. This reflects of dynamic response, possibly because of the longer interval of 0.40 seconds (corresponding to a 9 m wheel spacing) between the second and third axles, allowing oscillations to amplify.

Finally, the fourth axle is passed at 1.02 seconds, recording a minimum velocity of -0.71 m/s. Then, followed by a rebound peak of 1.41 m/s, resulting in the maximum amplitude of 2.12 m/s. After this final rebound, the velocity gradually stabilises toward zero, indicating the onset of damping effects that reduce soil oscillations. This damping behaviour is critical for railway substructure performance, as prolonged high-amplitude vibrations can contribute to track instability and long-term settlement.

Table 6 summarises the relationship between vertical velocity and dynamic time for all rails positioned over unreinforced soil with all rails located at 24 m in the Y direction. Train 1 is located at X = 1.775 m (Rail 1, R1) and X = 3.225 m (Rail 2, R2), while Train 2 is located at X = −1.775 m (Rail 3, R3) and X = −3.225 m (Rail 4, R4).

Table 6. Summary of the relationship between vertical velocity and dynamic time for all rails in unreinforced soil at 24 m in the Y direction.

Train	Rail	Axle	Min Velocity (m/s)	Mean of Minimum Velocity	Rebound Velocity (m/s)	Mean of Rebound Velocity	Amplitude after each axle (m/s)	Mean of Amplitude
Train 1	R 1	1	-1.56	-1.35	0.41	0.86	1.97	2.21
		2	-1.43		1.31		2.74	
		3	-1.69		0.32		2.01	
		4	0.71		1.41		2.12	
	R 2	1	-1.59	-1.58	0.49	0.88	2.08	2.46
		2	-1.98		1.26		3.24	
		3	-2.06		0.39		2.45	
		4	-0.68		1.37		2.05	
Train 2	R 3	1	-1.73	1.65	0.66	1.10	2.39	2.75
		2	-2.13		1.48		3.61	
		3	-1.91		0.54		2.45	
		4	-0.84		1.70		2.54	
	R 4	1	-1.47	1.36	0.46	0.94	1.93	2.77
		2	-1.51		1.25		2.76	
		3	-1.33		0.56		1.89	
		4	-1.14		1.47		2.61	

Note: Rail positions along the X-axis: R1 = 1.775 m, R2 = 3.225 m, R3 = -1.775 m, R4 = -3.225 m.

The downward velocity, which illustrates the maximum soil compression due to the axle load, varied across the rail positions. Under Train 1, the minimum downward velocity is -2.06

DOI: https://doi.org/10.17509/ijost.v10i2.83905
p- ISSN 2528-1410 e- ISSN 2527-8045

m/s, recorded under axle 3 of Rail 2 (R2). In contrast, the maximum downward velocity of -0.68 m/s is observed under axle 4 of (Rail 2) R2. Moreover, the mean downward velocity is -1.35 m/s under R1. However, it records as -1.58 m/s under R2. In Train 2, the minimum downward velocity of -2.13 m/s is recorded at axle 2 of R3. In contrast, the maximum downward velocity of -0.84 m/s is recorded under axle 4 of R3. In addition, R3 shows a mean downward velocity of -1.65 m/s, while R4 displays a noticeable reduction in the mean downward velocity to -1.36 m/s. Overall, the lowest value of −2.13 m/s occurs at R3 under Axle 2 of Train 2, whereas the higher minimum of −0.68 m/s is noted at R2 under Axle 4 of Train 1.

Rebound velocity, which describes the upward motion after a moving axle load, illustrates a significant variation. In Train 1, the mean rebound velocity is 0.86 m/s under R1, while it is recorded as 0.88 m/s under R2. In Train 2, R3 is noted to have a mean rebound velocity of 1.10 m/s, whereas R4 shows an obvious reduction in the mean rebound velocity to 0.94 m/s.

The maximum amplitude after each axle is 3.61 m/s, recorded at R3 under Axle 2, while a mean peak value of 2.77 m/s is observed at R4. The lowest amplitude, 2.93 m/s, is recorded at R4 under Axle 1, while the mean peak value of 2.21 m/s is observed at R1.

Table 7 presents the dynamic behaviour of subgrade soil reinforced with DMCs of 10 m length and 2 m spacing, based on vertical velocity measurements recorded along four rail positions (R1 to R4).

Table 7. The summary of relationships between vertical velocity and dynamic time for all rails in reinforced soil with DMCs of 10 m length and 2 m spacing at 25 m in the Y direction.

Train	Rail	Axle	Min Velocity (m/s)	Mean of Minimum Velocity	Rebound Velocity (m/s)	Mean of Rebound Velocity	Amplitude after each axle (m/s)	Mean of Amplitude
Train 1	R 1	1	-1.35	-1.49	0.95	1.02	2.30	2.50
		2	-1.62		1.25		2.87	
		3	-1.39		0.62		2.01	
		4	-1.60		1.25		2.85	
	R 2	1	-0.99	-1.31	1.02	1.03	2.01	2.34
		2	-1.43		1.22		2.65	
		3	-1.33		0.59		1.92	
		4	-1.50		1.28		2.78	
Train 2	R 3	1	-1.29	-1.36	0.77	1.06	2.06	2.41
		2	-1.64		1.32		2.96	
		3	-1.24		0.64		1.88	
		4	-1.25		1.49		2.74	
	R 4	1	-0.99	-1.35	0.79	0.86	1.79	2.19
		2	-1.47		1.05		2.52	
		3	-1.33		0.47		1.80	
		4	-1.59		1.07		2.66	

Note: Rail positions along the X-axis: R1 = 1.775 m, R2 = 3.225 m, R3 = -1.775 m, R4 = -3.225 m.

The measurements are taken at constant lateral (Y = 25 m) and vertical (Z = 1.75 m) coordinates, under two separate train loadings. The table reports the minimum vertical velocity, rebound velocity, and amplitude observed after each axle for each rail.

For Train 1, R1 exhibits the lowest mean minimum velocity (−1.49 m/s), indicating the smallest settlement compared to R2, which records −1.31 m/s. A similar trend is observed under Train 2, where R3 exhibits a lower mean minimum velocity (−1.36 m/s) than Rail 4 (R4) at −1.35 m/s.

DOI: https://doi.org/10.17509/ijost.v10i2.83905
p- ISSN 2528-1410 e- ISSN 2527-8045

Rebound velocity, which describes the upward motion resulting from elastic rebound after a moving axle load, illustrates a significant variation. In Train 1, the minimum rebound velocity is 0.59 m/s, recorded under axle 3 of R2. In contrast, the maximum rebound velocity of 1.28 m/s is noted under axle 4 of R1. In addition, the mean rebound velocity is 1.02 m/s under R1, while it is recorded as 1.03 m/s under R2. In Train 2, the minimum rebound velocity of 0.47 m/s is recorded at axle 3 of R4. However, the maximum rebound velocity of 1.49 m/s is noted under axle 4 of R3. Moreover, R3 is noted to have a mean rebound velocity of 1.06 m/s, whereas R4 shows an obvious reduction in the mean rebound velocity to 086 m/s.

The amplitude velocity, representing the period between the minimum and rebound velocity after each moving axle load, is presented in this table. For Train 1, the highest mean amplitude is observed in R1 at 2.5 m/s, followed by R2 at 2.34 m/s. In Train 2, R3 displays a higher mean amplitude (2.41 m/s) compared to R4 at 2.19 m/s.

When designing foundations under moving load scenarios, the amplitude velocity is considered a fundamental aspect for evaluating deformation and assessing the stability of the foundation [20]. The amplitude velocity, as illustrated in **Table 8**, is the difference between the minimum downward velocity and the maximum rebound velocity. It displays the average soil amplitudes at R1, R2, R3, and R4 for unreinforced soil and soil reinforced with DMCs of 10 m length at a 2 m spacing at 25 m in the Y direction. In addition, the soil was reinforced with DMCs of 10 m length at a 2 m spacing at 25.5 m in the Y direction.

Table 8. Average soil response amplitude (m/s) by rail position**.**

Rail	Unreinforced soil	Soil with DMC at 2m spacing	Soil with DMC at 3 m spacing
R 1	2.21	2.50	2.17
R 2	2.46	2.34	2.90
R 3	2.75	2.41	1.79
R 4	2.77	2.19	2.70
Mean of all rails	2.55	2.36	2.39

Under unreinforced soil, the highest amplitude velocity of 2.77 m/s is recorded under R4. In contrast, the lowest amplitude velocity is 2.21 m/s, noted at R1. It is also observed as 2.46 m/s under R2 and 2.75 m/s under R3. The mean of all rails is 2.55 m/s. Under soil reinforced with DMCs at a 2 m spacing when the location at 25 m in the Y direction, the amplitude velocity of 2.19 m/s under R4 is the lowest magnitude. However, it records the greatest value of 2.50 m/s at R1. The amplitude is noted as 2.34 m/s under R2 and 2.41 m/s under R3. The mean of all rails is 2.36 m/s. Under soil reinforced with DMCs at a 3 m spacing at 25.5 m in the Y direction, the highest amplitude velocity of 2.90 m/s is recorded under R2. In contrast, the lowest amplitude velocity is 2.17 m/s, recorded at R1. It is noted as 1.79 m/s under R3 and 2.70 m/s under R4. The mean of all rails is 2.39 m/s. Soil reinforced with DMCs at a 2 m spacing shows the smallest mean amplitude of 2.36 m/s. In contrast, the maximum mean amplitude (2.54 m/s) is observed under unreinforced soil conditions.

The effect of DMC length on soil response beneath Rail 1 is investigated by modelling DMCs of varying lengths, such as 7, 10 and 15 m at a steady spacing of 2 m when the location at 25 m in the Y direction. **Figure 12** shows the relationship between vertical soil velocity and dynamic time for each DMC length. For DMC design with a length under 7 m, the lowest recorded downward velocity under all axes is -1.78 m/s, while the maximum rebound velocity under all axes is 1.31 m/s. The amplitude velocity, which is the magnitude of the lowest downward velocity to the maximum rebound velocity, is shown in this figure. It records 3.09 m/s, presenting the soil deformation due to the moving load. When designing the DMCs with

DOI: https://doi.org/10.17509/ijost.v10i2.83905
p- ISSN 2528-1410 e- ISSN 2527-8045

a length under 10 m, this results in recording -1.62 m/s as the smallest downward velocity. In contrast, the peak value of rebound velocity is noted at 1.32 m/s, while the amplitude velocity is 2.94 m/s, indicating a slightly lower value compared to the DMCs configured with a 7 m length.

The effect of DMC length on soil response beneath Rail 1 is investigated by modelling DMCs of varying lengths, such as 7, 10 and 15 m at a steady spacing of 2 m when the location at 25 m in the Y direction. **Figure 12** shows the relationship between vertical soil velocity and dynamic time for each DMC length. For DMC design with a length under 7 m, the lowest recorded downward velocity under all axes is -1.78 m/s, while the maximum rebound velocity under all axes is 1.31 m/s. The amplitude velocity, which is the magnitude of the lowest downward velocity to the maximum rebound velocity, is shown in this figure. It records 3.09 m/s, presenting the soil deformation due to the moving load. When designing the DMCs with a length under 10 m, this results in recording -1.62 m/s as the smallest downward velocity. In contrast, the peak value of rebound velocity is noted at 1.32 m/s, while the amplitude velocity is 2.94 m/s, indicating a slightly lower value compared to the DMCs configured with a 7 m length.

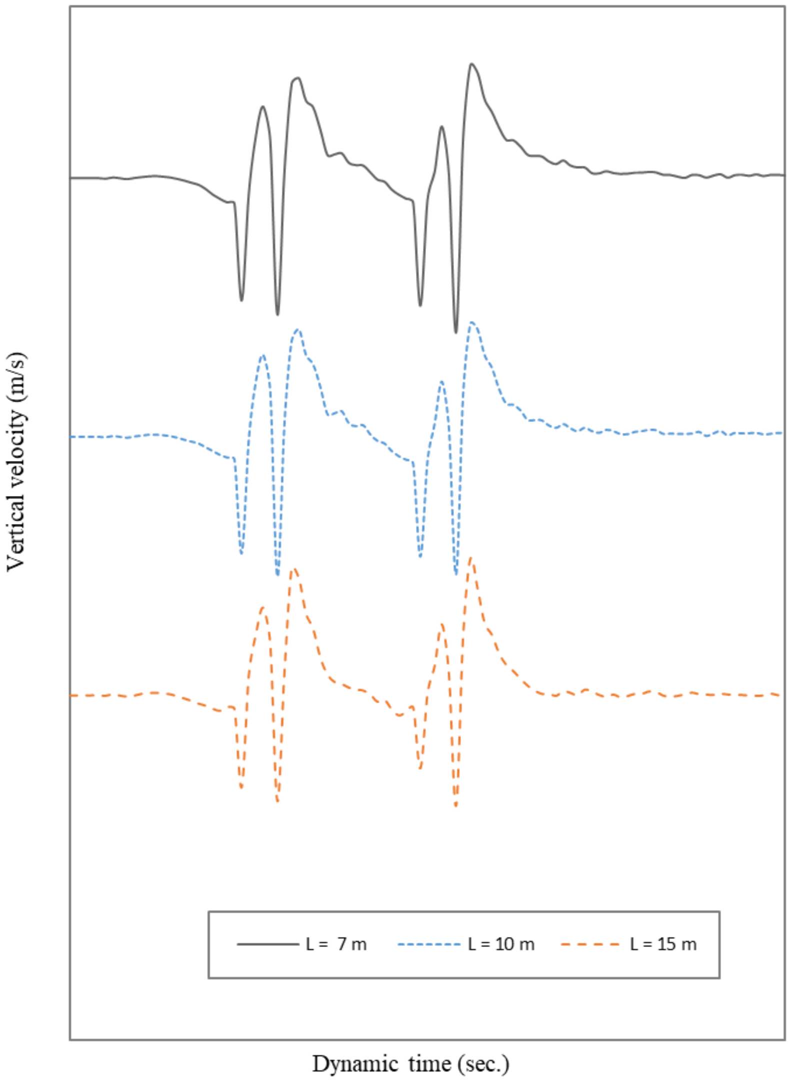

Figure 12. The influence of a moving train on the vertical velocity under Rail 1 when using DMCs at a 2 m spacing with different lengths.

DOI: https://doi.org/10.17509/ijost.v10i2.83905
p- ISSN 2528-1410 e- ISSN 2527-8045

For DMCs modelled with a length of 15 m, a lower downward velocity of -1.28 is recorded. The reduction ratio is about 39 % and 27 % compared with those designed with lengths under 7 and 10 m, respectively. The highest peak-to-peak amplitude velocity is 2.8 m/s. It is also the lowest value compared with other types of modelling. These results demonstrate that with an increase in the length of DMCs under uniform spacing, the peak-to-peak amplitude velocity is reduced, reflecting reduced soil settlement under moving loads.

Table 9 shows an elaborated comparison of the peak-to-peak amplitudes and details of the vertical velocity for unreinforced and reinforced soil using DMCs. The length of the DMCs differed (e.g., 10 and 15 m), and the spacing intervals between the centre to centres of the DMCs varied from 2 to 3 m. The results of this study are obtained from locations directly under Rails R1 and R2 of Train 1 and Rails R3 and R4 of Train 2.

As shown, the data of unreinforced soil is estimated when the rails are located at 25 in the Y axis. The amplitude velocity, which is illustrated and discussed in the results of Figure 12, is presented in this table. These are the results from the peak of the lowest downward velocity to the peak of the largest rebound velocity along all the moving rails. The amplitude velocity is 3.1 m/s under R1, 3.43 m/s under R2, 3.83 m/s under R3, and 3.51 m/s under R4. The mean amplitude of all rails is 3.47 m/s. in addition, mean amplitude of all rails is 3.47 m/s. In addition, the standard deviation and standard error are found to be 0.3 and 0.08, respectively, considering their relatively low values. This indicates that the data for the moving load under all rails is approximately around the mean.

When the soil is reinforced with DMCs under an L10S2 pattern, the average amplitude velocity (m/s) is recorded as 3.2 m/s, and the standard deviation and standard error for calculation of the mean (average) are 0.48 and 0.12, respectively. In addition, the ratio of reduction is approximately 7.8%. The lowest average amplitude velocity of 2.81 is recorded with modelling the DMCs under a L10S15 configuration, as well, and the ratio of reduction is approximately close to 18.91% compared to unreinforced soil. In contrast, the average amplitude ratio is noted as 7.37% and 3.86% of soil reinforced with DMCs using L10S3 and L15S3 formation, respectively. Although the ratio of average amplitude when using DMCs under 3 m spacing is lower than 2 m spacing, the result is still better than unreinforced soil.

Table 9. Effect of soil modelling on velocity amplitude of moving train at various positions along an adjacent rail track.

Soil modelling	Y - direction (m)	Peak-to-peak amplitude of velocity (m/s)				Average amplitude velocity (m/s)	Average Amplitude Ratio (%)
		Rail					
		1	2	3	4		
Soil	24	3.10	3.43	3.83	3.51	3.47	--
L10S2	25	2.94	2.84	3.13	3.89	3.20	7.80
L15S2	25	2.87	2.37	2.63	3.39	2.81	18.91
L10S3	25.5	3.01	2.83	3.17	3.83	3.21	7.37
L15S3	25.5	3.41	3.12	2.91	3.89	3.33	3.86

4. CONCLUSION

The design and construction of a moving heavy-haul train on loose sand soil supported by DMCs can be evaluated using Plaxis 3d by calibrating and adjusting historical data from experimental tests on silty sand with low relative density. The novelty of this study fills a gap in the literature concerning the movement of trains over embankments constructed on soil

DOI: https://doi.org/10.17509/ijost.v10i2.83905
p- ISSN 2528-1410 e- ISSN 2527-8045

strengthened by DMCs. Previous research has focused on soil improvement under static loads of trains or moving trains above embankments without the use of DMCs.

Based on the results of adjacent train movements in the same direction, soil reinforced with DMCs significantly reduced settlement under static loads. The effectiveness of DMCs increases with their length and reduced spacing. Specifically, using DMCs with a 15 m length and 2 m spacing (L15S2) achieved the most significant settlement reduction, improving the settlement ratio by 41% compared to untreated soil. This enhancement is attributed to increased skin friction and the DMCs transitioning from a 'floating' to an 'end-bearing' state.

The investigation of movement conditions also revealed that DMCs significantly reduce soil settlement beneath a moving train. The average settlement decreases from 87 mm in untreated soil to 54 mm when reinforced with 10 m long DMCs spaced 2 m apart. Increasing the length of the DMCs from 10 to 15 m improves the Settlement Reduction Ratio (SRR) from 38 to 50%. However, the SRR decreases from 38 to 28% when spacing increases from 2 to 3 m for 10 m long DMCS and from 50 to 32% for 15 m long DMCS with the same spacing. The minimum SRR is 17% for a 10 m long DMCS spaced 3 m apart at a location between the DMCs. Increasing the DMC length to 15 m raises the SRR to 26% for the same spacing and positions.

Moreover, the vertical velocity analysis indicated notable dynamic soil responses characterised by compression and rebound cycles, directly influenced by axle spacing and train velocity. The highest vertical velocity amplitudes were recorded in unreinforced soil conditions, particularly beneath the inner rails, emphasising greater soil deformation under direct axle loads. Reinforcing soils with DMCS consistently reduced these amplitudes, indicating improved dynamic stability. Notably, a 2 m DMC spacing yielded the most efficient outcome, effectively balancing performance.

Overall, the optimised use of DMCs significantly enhances subgrade performance under dynamic loading, ensuring reduced settlements and improved stability, critical for maintaining long-term railway integrity and safety.

5. ACKNOWLEDGMENT

The authors would like to thank Mustansiriyah University (www.uomustansiriyah.edu.iq), Baghdad, Iraq, for its support in the present work.

6. AUTHORS' NOTE

The authors declare that there is no conflict of interest regarding the publication of this article. The authors confirmed that the paper was free of plagiarism.

7. REFERENCES

[1] Bouassida, M., Fattah, M. Y., and Mezni, N. (2022). Bearing capacity of foundation on soil reinforced by deep mixing columns. *Geomechanics and Geoengineering*, *17*(1), 309-320.

[2] Hessouh, J. J., Eslami, J., Beaucour, A. L., Noumowe, A., Mathieu, F., and Gotteland, P. (2023). Physical and mechanical characterisation of deep soil mixing (DSM) materials: Laboratory vs construction site. *Construction and Building Materials*, *368*, 130436.

[3] Al-Qaisi, M. S., and Al-Waily, M. J. M. (2022). Experimental Study of Soft Clay Soil Improvement by Deep Mixing Method. *Mathematical Modelling of Engineering Problems*, *9*(1), 224-232.

[4] Esmaeili, M., Gharouni-Nik, M., and Khajehei, H. (2014). Evaluation of deep soil mixing efficiency in stabilizing loose sandy soils using laboratory tests. *Geotechnical Testing Journal*, *37*(5), 817-827.

[5] Saberian, M., Moradi, M., Vali, R., and Li, J. (2018). Stabilized marine and desert sands with deep mixing of cement and sodium bentonite. *Geomechanics and engineering*, *14*(6), 553-562.

[6] Esmaeili, M., and Khajehei, H. (2016). Mechanical behavior of embankments overlying on loose subgrade stabilized by deep mixed columns. *Journal of Rock Mechanics and Geotechnical Engineering*, *8*(5), 651-659.

[7] Bolton, M., Noonan, J., and Oh, E. (2016). Effect of soil cement column spacing and area replacement ratio on embankment bearing capacity: A Queensland case study. *GEOMATE Journal*, *11*(26), 2589-2594.

[8] Dehghanbanadaki, A., Motamedi, S., and Ahmad, K. (2020). FEM-based modelling of stabilized fibrous peat by end-bearing cement deep mixing columns. *Geomechanics and Engineering*, *20*(1), 75-86.

[9] Hasan, H. A., Hacheem, Z. A., Almurshedi, A. D., and Khabbaz, H. (2023). The influence of styrene butadiene latex on sandy soil reinforced by soil mixed columns under raft foundation. *Mathematical Modelling of Engineering Problems, 10*(3), 733-739.

[10] Do, T., Gunnvard, P., Mattsson, H., and Laue, J. (2021, April). Railway embankment behaviour due to increased axle loads-A numerical studyIn *IOP Conference Series: Earth and Environmental Science, 710*(1), 012040.

[11] Hadi, M. A., and Alzabeebee, S. (2023). Development of a finite element model to study the settlement of ballasted railway tracks subjected to two adjacent moving trains. *Transportation Infrastructure Geotechnology*, *10*(5), 733-748.

[12] Likitlersuang, S., Pholkainuwatra, P., Chompoorat, T., and Keawsawasvong, S. (2018). Numerical modelling of railway embankments for high-speed train constructed on soft soil. *Journal of GeoEngineering*, *13*(3), 149-159.

[13] Farouk, A., and Shahien, M. M. (2013). Ground improvement using soil–cement columns: Experimental investigation. *Alexandria Engineering Journal*, *52*(4), 733-740.

[14] Chalabii, J., Movahedi Rad, M., and Hosseini, S. (2023). Optimal shape design of concrete sleepers under lateral loading using DEM. *Buildings*, *13*(7), 1574.

[15] Shahraki, M., Sadaghiani, M. R. S., Witt, K. J., and Meier, T. (2014). 3d modelling of train induced moving loads on an embankment. *Plaxis Bulletin*, *36*(2014), 10-15.

[16] Dižo, J., Blatnický, M., and Pavlík, A. (2018). Process of modelling the freight wagon multibody system and analysing its dynamic properties by means of simulation computations. *MATEC Web of Conferences*, *235*, 00027.

[17] Pintão, B., Mosleh, A., Vale, C., Montenegro, P., and Costa, P. (2022). Development and validation of a weigh-in-motion methodology for railway tracks. *Sensors*, *22*(5), 1976.

[18] Bosso, N., Magelli, M., and Zampieri, N. (2023). Dynamical effects of the increase of the axle load on European freight railway vehicles. *Applied Sciences*, *13*(3), 1318.

DOI: https://doi.org/10.17509/ijost.v10i2.83905
p- ISSN 2528-1410 e- ISSN 2527-8045

[19] Bolton, M., Noonan, J., and Oh, E. (2016). Effect of soil cement column spacing and area replacement ratio on embankment bearing capacity: A Queensland case study. *GEOMATE Journal*, *11*(26), 2589-2594.

[20] Lazorenko, G., Kasprzhitskii, A., Khakiev, Z., and Yavna, V. (2019). Dynamic behavior and stability of soil foundation in heavy haul railway tracks: A review. *Construction and Building Materials*, *205*, 111-136.

DOI: https://doi.org/10.17509/ijost.v10i2.83905
p- ISSN 2528-1410 e- ISSN 2527-8045